Journal of Geodesy (2004) 78: 386–392
DOI 10.1007/s00190-004-0418-x

Journal of Geodesy

Surface gravitational field and topography changes induced by the Earth's fluid core motions

M. Greff-Lefftz[1], M. A. Pais[2], J.-L. Le Mouël[1]

[1] Institut de Physique du Globe de Paris, Département de Géomagnétisme et Paléomagnétisme, 4 place Jussieu, 75252 Paris 05, France
e-mail: greff@ipgp.jussieu.fr
[2] Departamento de Fisica, Universidade de Coimbra, Rua Larga, 3004-516 Coimbra, Portugal

Received: 12 September 2003 / Accepted: 14 July 2004 / Published online: 16 November 2004

Abstract. Using a Love number formalism, the elastic deformations of the mantle and the mass redistribution gravitational potential within the Earth induced by the fluid pressure acting at the core–mantle boundary (CMB) are computed. This pressure field changes at a decadal time scale and may be estimated from observations of the surface magnetic field and its secular variation. First, using a spherical harmonic expansion, the poloidal and toroidal part of the fluid velocity field at the CMB for the last 40 years is computed, under the hypothesis of tangential geostrophy. Then the associated geostrophic pressure, whose order of magnitude is about 1000 Pa, is computed. The surface topography induced by this pressure field is computed using Love numbers, and is a few millimetres. The mass redistribution gravitational potential induced by these deformations and, in particular, the zonal components of the related surface gravitational potential perturbation (ΔJ_2, ΔJ_3 and ΔJ_4 coefficients), are calculated. Overall perturbations for the J_2 coefficient of about 10^{-10}, for J_3 of about 10^{-11} and for J_4 are found of about 0.3×10^{-11}. Finally, these theoretical results are compared with recent observations of the decadal variation of J_2 from satellite laser ranging. Results concerning ΔJ_2 can be described as follows: first, they are one order of magnitude too small to explain the observed decadal variation of J_2 and, second, they show a significant linear trend over the last 40 years, whose rate of decrease amounts to 7% of the observed value.

Key words: Core–mantle boundary (CMB) flows – Geostrophic pressure – Elasto-gravitational deformation

Correspondence to: M. Greff-Lefftz

1 Introduction

According to space geodetic observations over the past 25 years, the zonal degree-2 coefficient of the Earth's gravitational potential (J_2), which is related to the Earth's dynamic oblateness, decreased until around 1998, followed by an increasing trend until 2002 (Cox and Chao 2002) and, finally, a decrease from that time to the present (Chao et al. 2003). These recent observations bring out decadal variations in J_2 superimposed on the secular decrease associated with postglacial rebound. Cox and Chao (2002) discussed several mechanisms related to the melting of glaciers or polar ice caps which could be able to explain these observations; none of these provides a satisfactory answer, however.

Cazenave and Nerem (2002) concluded that, because of the magnitude of the event, only two potential candidates remain: masses moving in the fluid outer core or in the oceans. A recent study by Cox et al. (2003) compared the oceanographic signals with satellite laser ranging (SLR)-derived gravity observations. Because the timing of the J_2 anomaly onset corresponds with the last big El Niño event, they concluded that the most consistent explanation of the observed J_2 anomaly is an oceanic cause. Here, we discuss the influence of the Earth's fluid core motions on the decadal variations of the gravitational field at the Earth's surface. We use a mechanism in which the fluid overpressure field at the core–mantle boundary (CMB) changes and induces time-dependent deformations in the mantle. In a similar study, Fang et al. (1996) found that the CMB geostrophic pressure, derived from 'frozen flux' core surface flow estimates at epochs 1965 and 1975, produces a significant contribution to the time variation of the J_2 coefficient—about 50% of the observed $\dot{J}_2$. They subtracted the deformation at the 1965 epoch from its counterpart at the 1975 epoch. Consequently, they could not separate the decadal contribution from the secular one in the induced J_2 variation. Dumberry and Bloxham

(2003) found that the variations in the Earth's gravitational field induced by pressure changes at the CMB caused by torsional oscillations in the core are weak in comparison with the decadal observations. Here, we are interested in simultaneously investigating both secular and decadal variations of the surface elasto-gravitational deformations induced by pressure changes at the CMB. We compute a time-dependent pressure field derived from core surface flow estimates based on a recent geomagnetic field model spanning the last 40 years (Sabaka et al. 2002). This time-dependent model takes into account satellite data as well as data from ground-based observatories.

This paper is organized as follows. In the first part (Sect. 2), we briefly review the method used to compute the fluid flow at the CMB from surface observations of the geomagnetic field. We then compute the changes in the axial angular momentum of the core, for the last 40 years, associated with these motions. In Sect. 3, we derive the geostrophic pressure associated with these motions and, solving the elasto-gravitational equations, we compute the associated surface deformations using a Love number formalism. Finally, we investigate (in Sect. 4) the temporal evolution of the zonal coefficients of the gravitational potential and we compare these results with recent geodetic observations.

2 Computation of the tangential flow at the CMB

The tangential flow at the CMB ($\boldsymbol{v}_H$) can be obtained from surface magnetic field data and core dynamics approximations. From observations of the magnetic field and its secular variation near the Earth's surface, spherical harmonic models are computed. If we assume that the mantle is an insulator, these magnetic field models may be downward-continued to the bottom of the mantle.

Within the fluid core, the magnetic induction equation relates the time variation of the magnetic field to terms that represent advection of the field by the flow and magnetic diffusion

$$\frac{\partial \boldsymbol{B}^c}{\partial t} = \boldsymbol{\nabla} \wedge \left(\boldsymbol{v} \wedge \boldsymbol{B}^c\right) + \eta \Delta \boldsymbol{B}^c \tag{1}$$

where $\boldsymbol{B}^c$ is the magnetic field within the core, $\boldsymbol{v}$ is the fluid velocity and η is the magnetic diffusivity. For time scales of a few decades, the diffusion can be considered negligible with respect to the advection term: this is the so-called frozen flux approximation (Roberts and Scott 1965). In the frozen flux approximation, the radial component of the induction equation links the radial magnetic field B_r^c with the tangential flow $\boldsymbol{v}_H$ at the CMB

$$\frac{\partial B_r^c}{\partial t} = -\boldsymbol{\nabla}_H.(\boldsymbol{v}_H B_r^c) \tag{2}$$

The radial magnetic field B_r^c is continuous across the CMB and, consequently, from observations of the secular variation of the radial magnetic field at the Earth's surface, we can compute the horizontal divergence of $\boldsymbol{v}_H B_r^c$ within the fluid core at the CMB. At this stage, we have one equation and two unknowns, namely the two components of the tangential flow velocity. Consequently, we need further constraints. In our study, we assume that the flow at the CMB is tangentially geostrophic, i.e. there exists an equilibrium between the horizontal gradient of the pressure P^c and the Coriolis force, with the Lorentz force being presumably negligible at the CMB and the buoyancy force being mostly radial (Le Mouël 1984)

$$2\rho^c \left(\boldsymbol{\Omega} \wedge \vec{v}\right)_H = -\boldsymbol{\nabla}_H P^c \tag{3}$$

where $\boldsymbol{\Omega}$ is the sidereal rotation rate of the Earth and ρ^c is the density of the fluid core at the CMB, which is assumed to be uniform. This force balance [Eq. (3)] implies the following condition on the flow at the CMB:

$$\boldsymbol{\nabla}_H \cdot (\cos\theta\, \boldsymbol{v}_H) = 0 \tag{4}$$

where θ is the colatitude. A further condition is required in order to obtain a unique solution, which is generally the hypothesis of a large-scale flow. This condition enters as a regularization term in the inversion procedure; for more details, see Pais and Hulot (2000).

Using Eqs. (2) and (4) and the observed secular variation of the surface magnetic field, we have thus determined a large-scale $\boldsymbol{v}_H$ at the CMB. This velocity flow at the CMB is classically expanded into poloidal and toroidal spherical harmonic vectors (see e.g. Gubbins and Roberts 1987). In this study, we are essentially interested in the zonal toroidal motions within the core. These motions are expanded in spherical harmonics in the following way:

$$\vec{v}_{\mathrm{zon}} = -\sum_{n=1}^{\infty} \tau_n^0 \;\partial_\theta P_n^0(\cos(\theta))\vec{e_\varphi} \tag{5}$$

where P_n^0 are the Legendre polynomials and τ_n^0 the zonal toroidal coefficients in km/year relative to the mantle. These motions do not depend on the longitude. Following Jault et al. (1988), we assume that exchanges of angular momentum between the core and the mantle are carried, inside the core, by flows organized in cylinders that are coaxial with the rotation axis. The flow in Eq. (5) can then be interpreted as the core-surface expression of those cylinders.

To compute these motions, we use the magnetic field model derived by Sabaka et al. (2002, submitted). This is a time-dependent model that spans the last 40 years (1960–2000), taking into account satellite data (POGO, Magsat, OERSTED, CHAMP) as well as data from ground-based observatories. Figure 1 shows the temporal evolution, in km/year, of the low-degree coefficients τ_n^0 for n = 1–5. The amplitude is of the order of 1–10 km/year. From Fig. 1, there is a significant secular trend in τ_1^0, which is sometimes related to the classical westward drift of the core with respect to the mantle for the last 30 years. This behaviour is interesting, as it has significant implications for the present study, as we will see below. A decreasing trend in τ_1^0, starting around 1970, could already be seen in previous core-fluid-flow inversions [such as those using the *ufm1* model of

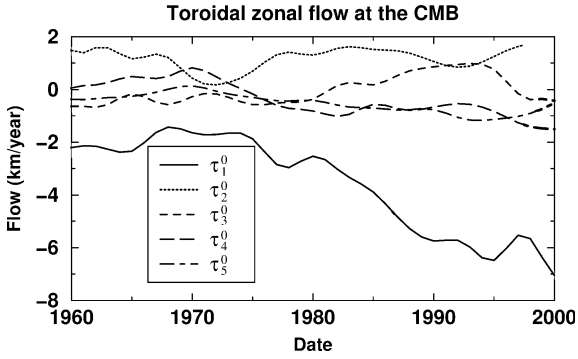

Fig. 1. Zonal coefficients of the toroidal flow at the CMB as a function of time

Bloxham and Jackson (1992)], but our result shows a stronger trend based on more recent data. For example, we obtain an average $\tau_1^0 \simeq -4.79$ km/year for 1980–2001. In comparison, Hulot et al. (2002) obtained a similar mean secular variation between 1980 and 2000 using the difference between data from the OERSTED (2000) and Magsat (1980) satellites: their secular variation model is consistent with an average $\tau_1^0 \simeq -4.87$ km/year (Eymin, pers. commun. 2003).

Before computing the elastic deformations, we will test our estimate of the zonal toroidal flow by evaluating the associated core angular momentum. Assuming that the CMB zonal flows are the core-surface expression of coaxial fluid cylinders rotating rigidly relative to each other, the changes in the axial angular momentum of the core (denoted by H_3^c) carried by these simple flows may be written as (see e.g. Jault et al. 1988; Greff-Lefftz and Legros 1995)

$$H_3^c = \frac{8\pi}{15}\rho^c b^5[\tau_1^0 + \frac{12}{7}\tau_3^0] \tag{6}$$

where b is the CMB radius (3480 km). We compare this core angular momentum with the decadal changes in the axial angular momentum of the mantle (denoted by H_3^m) computed from length-of-day (LOD) observations provided by the International Earth Rotation Service (IERS)

$$H_3^m = C^m \delta\Omega \tag{7}$$

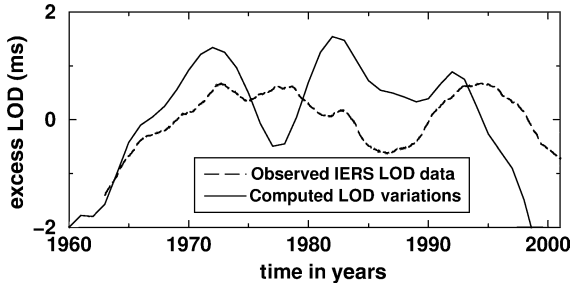

Fig. 2. Decadal changes in the LOD induced by fluid core motions (*solid line*) and in the observed LOD (*dashed line*) from IERS data

where C^m is the axial moment of inertia of the mantle and $\delta\Omega$ is the observed variation of the axial angular velocity of the Earth. The decadal excesses in LOD, both computed (i.e. $H_3^c \frac{2\pi}{C^m\Omega^2}$) and observed, are plotted in Fig. 2. Note that for the new magnetic field model derived by Sabaka et al. (submitted) and used in our study, we obtain the classical correlation between decadal LOD variations and modelled core angular momentum. That is, the decadal LOD fluctuations can be attributed to exchanges of angular momentum between the core and the mantle [for a review, see the web site of the Special Bureau for the Core of the IERS Global Geophysical Fluids Centre (GGFC): http://www.astro.oma.be/SBC]. We do not discuss the coupling mechanisms here, but it seems that a mixture of electromagnetic, topographic and gravitational are the most likely candidates (see e.g. Jault 2003).

3 Geostrophic pressure and elasto-gravitational deformations

Once we have computed a tangentially geostrophic flow at the CMB, we can compute the related geostrophic pressure P^c at the CMB using Eq. (3) (Gire and Le Mouël 1990). This pressure field is not stationary, and time variations can reach about 1000 Pa over 40 years. A snapshot is plotted in Fig. 3a for 1980. The zonal

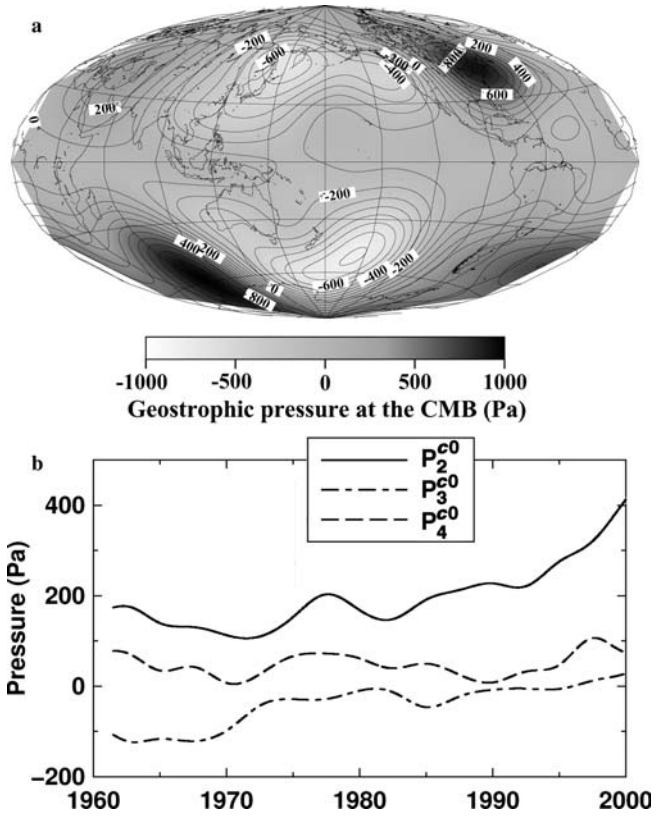

Fig. 3. **a** Snapshot of the geostrophic pressure field at the CMB for 1980 computed from the tangential flow at the CMB derived by Hulot et al. (1990); **b** Temporal evolution of the zonal coefficients of the pressure: P_2^{c0} (*solid line*), P_3^{c0} (*dot-dashed line*) and P_4^{c0} (*dashed line*)

coefficients of the CMB geostrophic pressure are computed in the following way (Gire and Le Mouël 1990):

$$P_n^{c0} = -2\rho^c \Omega b \left[\frac{n-1}{2n-1} \tau_{n-1}^0 + \frac{n+2}{2n+3} \tau_{n+1}^0 \right] \quad (8)$$

Figure 3b shows the temporal evolution of the low-degree zonal coefficients. For P_2^{c0} in Fig. 3, the magnitude of the pressure variation is a few hundred Pascal (Pa).

Let us point out that the large-scale assumption solves, in a somewhat 'brute force' way, a non-uniqueness problem that otherwise would still exist. It can be shown (e.g. Backus and Le Mouël 1986; Chulliat and Hulot 2000) that the solution to Eq. (2), subject to the constraint given by Eq. (3), does not depend on adding an arbitrary value to P^c, which is constant on a connected-level curve of $\zeta = \frac{B_r}{\cos\theta}$. Moreover, this arbitrary constant can change from one connected-level curve to another. Therefore, there remains a pressure component associated with the CMB flow that cannot be determined from satellite observations and, consequently, is not taken into account in this study.

We now compute the elasto-gravitational deformations induced by the geostrophic pressure field. To do this, we solve the classical elasto-gravitational equations (Alterman et al. 1959) which consist of mass conservation, the momentum equation and the Poisson equation. Concerning the rheological laws for the mantle and the core, we assume that the mantle is elastic and that the core is an inviscid fluid. We write the boundary conditions so that they take into account the excitation source, which is here taken to be a pressure acting at the CMB (for more details, see Appendix A of Greff-Lefftz et al. 2000). The solutions are expanded in spherical harmonics up to degree and order $n_{\max} = 13$ and written using a Love number formalism. Within this formalism, each coefficient of degree n and order m of the radial displacement u_r and of the perturbation of the gravitational potential Φ_1 at the Earth's surface is proportional to the pressure coefficient of the same degree n and order m. The proportionality coefficient is a Love number $\overline{h}_n^1$ or $\overline{k}_n^1$ following the nomenclature used by Hinderer and Legros (1989)

Table 1. Love numbers used in this study

Degree n	$\overline{h}_n^1$	$\overline{k}_n^1$
2	0.23026	0.11160
3	0.10653	0.03306
4	0.05136	0.01156

$$u_r(a,\theta,\varphi) = \sum_{n=2}^{n_{\max}} \sum_{m=0}^{n} u_{rn}^m Y_n^m(\theta,\varphi) \quad \text{and } u_{rn}^m = \overline{h}_n^1 \frac{P_n^{cm}}{\rho g} \quad (9)$$

$$\Phi_1(a,\theta,\varphi) = \sum_{n=2}^{n_{\max}} \sum_{m=0}^{n} \Phi_{1n}^m Y_n^m(\theta,\varphi) \quad \text{and } \Phi_{1n}^m = \overline{k}_n^1 \frac{P_n^{cm}}{\rho} \quad (10)$$

where a is the Earth's radius, ρ the average density and g the surface gravity.

The gravity on the deformed surface of the Earth may be computed using $\overline{h}_n^1$ and $\overline{k}_n^1$

$$\delta g = \sum_{n=2}^{n_{\max}} \sum_{m=0}^{n} \left[-(n+1)\overline{k}_n^1 + 2\overline{h}_n^1 \right] \frac{P_n^{cm}}{\rho a} \quad (11)$$

We do not take into account the degree $n = 1$ coefficient in the computation of the elasto-gravitational

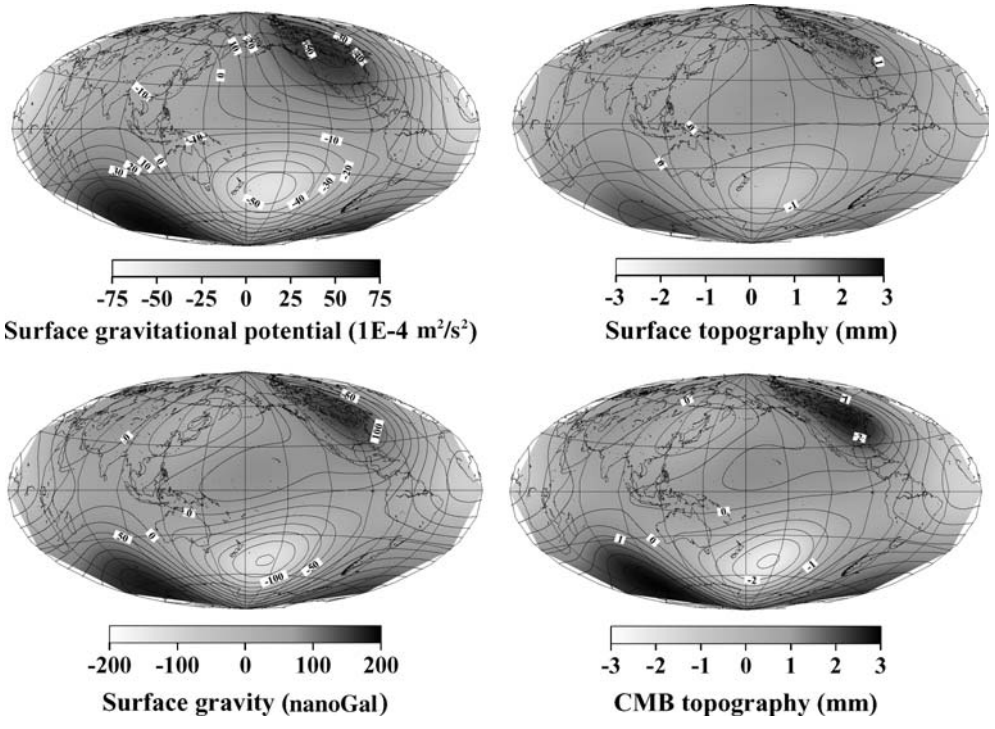

Fig. 4. A 'snapshot' of the surface gravitational potential, surface gravity and radial topography at the Earth's surface and at the CMB induced by the geostrophic pressure for 1980

deformations, because a degree-one pressure acting at the CMB cannot exist alone. In fact, the total force acting on the Earth must be equal to zero in order to conserve the centre of mass. This consequently imposes a relation between the degree-one coefficients of the pressures and tangential tractions acting on each fluid–solid interface of the model [inner-core boundary (ICB), CMB and outer surface–atmosphere boundary]. More details about this particular case can be found in Greff-Lefftz and Legros (1997).

We compute the pressure Love numbers for the PREM model (Dziewonski and Anderson 1981). The values for the low degrees are given in Table 1. Using these Love numbers, we compute and plot in Fig. 4 snapshots of the surface gravitational potential, the surface gravity, and the radial displacement at the CMB and at the Earth's surface induced, for example, by the geostrophic pressure for 1980. The amplitude of the induced surface gravity is about 100 nanoGal. The order of magnitude of the topography is a few millimetres; the radial displacement is two times larger at the CMB than at the surface.

4 Temporal evolution of ΔJ_n coefficients

We would now like to point out some results concerning the temporal evolution of the surface zonal harmonics of the gravitational potential. The perturbation of the zonal degree-n gravitational potential coefficient, called ΔJ_n, may be computed from the zonal degree-n pressure at the CMB

$$\Delta J_n = -\overline{k}_n^1 \frac{P_n^{c0}}{\rho g a} \tag{12}$$

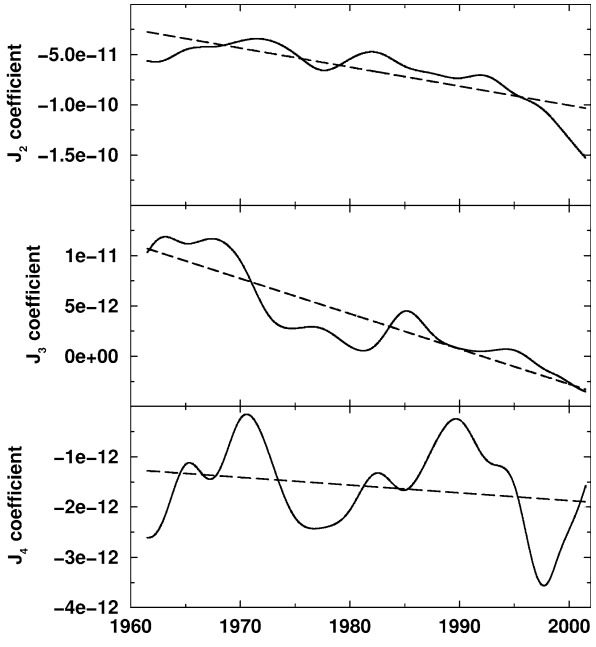

Fig. 5. Predicted temporal evolution of the zonal coefficients of the gravitational potential: ΔJ_2 (**top**), ΔJ_3 (**middle**) and ΔJ_4 (**bottom**) (*solid lines*); and linear regression of these curves (*dashed lines*)

ΔJ_n and P_n^{c0} consequently have the same temporal evolution. Figure 5 shows the temporal evolution of computed ΔJ_2, ΔJ_3 and ΔJ_4 between 1960 and 2002 (solid lines), and the linear regression of these curves (dashed lines). The amplitudes of the computed variations are $10^{-10}, 10^{-11}$ and 0.3×10^{-11} for $\Delta J_2, \Delta J_3$ and ΔJ_4, respectively. These variations are essentially decadal, but there are linear trends associated with secular terms of the zonal toroidal coefficients. This is particularly true for ΔJ_2, which is associated with the decreasing trend of τ_1^0 (see Fig. 1). We obtain for the slopes of the curves $\Delta \dot{J}_2 = -1.9 \times 10^{-12}$/year, $\Delta \dot{J}_3 = -3.5 \times 10^{-13}$/year and $\Delta \dot{J}_4 = -1.5 \times 10^{-14}$/year.

We compare these results with recent observations of decadal variations of J_2 from SLR data from 1979 to 2002 (Cox and Chao 2002). The top of Fig. 6 shows the observed J_2 (solid line) given by Cox and Chao (2002). We make a running average (with a length of average of about two years) of this curve and obtain the decadal and secular variation of J_2 (dot-dashed line). From a linear regression (thick solid line), we find a secular term of about $\dot{J}_2 \simeq -2.2 \times 10^{-11}$/year for the period 1980–2001. Note that, because of the nonlinearity of J_2 variation, the slope can vary depending on the period fitted. For this period, the uncertainty for the J_2 rate in the comprehensive solution is 0.4×10^{-11}/year (Cox and Chao 2002). The difference between the dot-dashed and

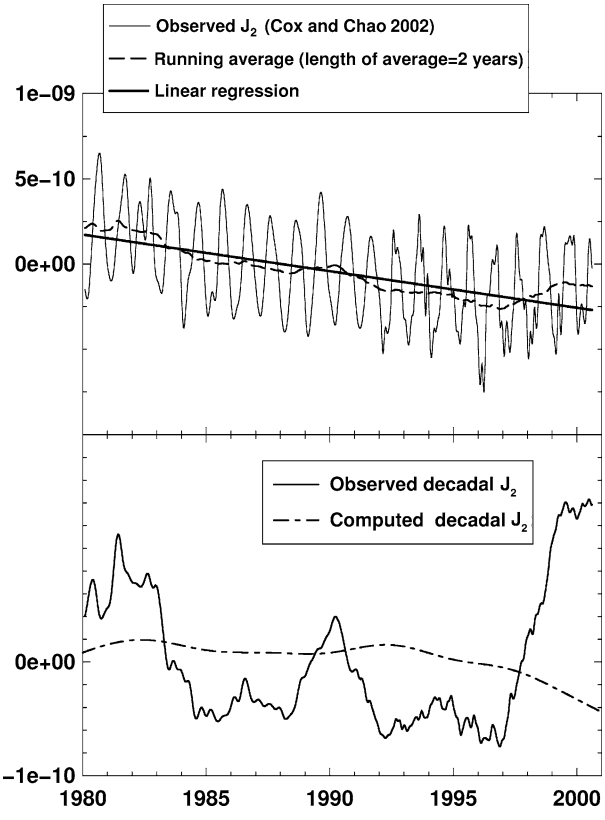

Fig. 6. Top: observed temporal variation of the J_2 coefficient from Cox and Chao (2002); **bottom**: comparison between the observed decadal variation of J_2 (*solid line*) and the computed ΔJ_2 (*dash-dot line*) induced by the zonal degree-two geostrophic pressure plotted in Fig. 3b

the thick solid curves is plotted at the bottom of Fig. 6 (solid line); it represents the observed decadal variations of J_2. These variations can amount to 2×10^{-10} in just a few years.

We apply the same treatment (i.e. running average and linear regression) for the computed ΔJ_2 induced by the geostrophic flow at the CMB. There is a secular term of about -0.19×10^{-11}/year. This value seems to be consistent with other recent models of secular variation of the magnetic field. This is a very interesting result, although it is smaller than the uncertainty for the observed J_2 rate: at least during the last 40 years, there is 7% of the observed value of $\dot{J}_2$ that can be attributed to the zonal toroidal flow at the CMB. As far as we are aware, this term has never been taken into account: the observed $\dot{J}_2$ (observed only over the past 25 years) is classically assumed to be essentially induced by the last deglaciation, melting of glaciers, and is partly by mantle convection, and is interpreted in terms of mantle viscosity (see e.g. Forte and Mitrovica 2001).

Estimates of the observed values of $\dot{J}_3$ and $\dot{J}_4$ from the EIGEN-1S data set [a reasonably recent gravity field model including CHAMP data; Reigber et al. (2002)] are $\dot{J}_3 = 0.6 \times 10^{-11}$/year and $\dot{J}_4 = -0.2 \times 10^{-10}$/year with very large uncertainties (50%). We can consequently conclude from our study that fluid core motions have a negligible contribution to the observed values for $\dot{J}_3$ and $\dot{J}_4$ coefficients.

Finally, we compare (bottom of Fig. 6) the observed (solid line) and computed (dot-dashed line) decadal variation of J_2, after the linear trends have been subtracted. This shows that the decadal variations of ΔJ_2, inferred from the fluid core motion, are too small to explain the observed oscillations, especially the large anomalous increase in J_2 after 1997, as reported by Cox and Chao (2002).

5 Summary and conclusion

First, we computed the CMB fluid flows responsible for the main decadal magnetic field variations at the Earth's surface, in a tangentially geostrophic approximation. The main geomagnetic field model used in the inversion is a new model for the time-dependent main field that spans the last 40 years and takes advantage of precise satellite data as well as ground-based observations (Sabaka et al. 2002, submitted). Second, we solved the classical elasto-gravitational equations to compute the surface gravitational potential and topography deformations induced by the previously computed flow-more precisely by the component that can be inferred from surface geomagnetic observations. We considered, in particular, the perturbations in the zonal gravitational potential coefficients induced by the zonal toroidal components of the flow.

We compared the estimated perturbation in ΔJ_2 with recent SLR observations, since there are speculations that the observed anomaly in the J_2 trend starting in 1998 could partly be attributed to the CMB flow (Cox and Chao 2002). Based on the present study's results, we conclude that the perturbations in J_2 induced by the zonal toroidal motions at the CMB are an order of magnitude too small to explain the observed decadal variation of J_2. Our results agree with those of Dumberry and Bloxham (2003), who investigated the variations in Earth's gravitational field induced by pressure changes at the CMB caused by torsional oscillations in the core. Similarly to this study, they concluded that the associated decadal time variation in J_2 is too weak to explain the observations.

A second important result of our study is the computation of a significant linear trend of ΔJ_2 induced by toroidal motions within the core. Fang et al. (1996), with a similar theoretical approach, computed the ΔJ_2 coefficient induced by geostrophic pressure at the CMB for two given years: 1965 and 1975. From the difference between the two obtained values, they proposed a very large $\Delta \dot{J}_2 = -1.3 \times 10^{-11}$/yr. As we can see from Fig. 5, the slope of the J_2 curve is strongly dependent on the period fitted, and consequently it is difficult to compare the Fang et al. (1996) results (obtained with two values) with our results (obtained with a 40-year continuous time series).

The $\dot{J}_2$ observed over the past 25 years is usually assumed to result from postglacial rebound and mantle convection, which are processes evolving at geological time scales. From this study, we conclude that there may be a significant contribution ($\simeq 7\%$) at a decadal time scale, resulting from zonal toroidal tangential flow at the CMB.

Acknowledgements. The authors thank C. Cox and B.F. Chao for providing data on the temporal evolution of J_2 and T. Sabaka for providing subroutines for evaluating the time-dependent main field model. M.A. Pais is supported by funds from FEDER/European Union and Fundação para a Ciência e Tecnologia/Portugal (POCTI/42023/CTA/2001). This study is IPGP contribution no. 1967.

References

Alterman Z, Jarosch H, Pekeris CH (1959) Oscillation of the Earth. Proc R Soc Lond A252:80–95

Backus GE, Le Mouël J-L (1986) The region on the core–mantle boundary where a geostrophic velocity field can be determined from frozen-flux magnetic data. Geophys J R Astr Soc 85:617–628

Bloxham J, Jackson A (1992) Time-dependent mapping of the magnetic field at the core–mantle boundary. J Geophys Res 97:19 537–19 564

Cazenave A, Nerem S (2002) Redistributing Earth's mass. Science 297:783–784

Chao BF, Au AY, Boy J-P, Cox CM (2003) Time-variable gravity signal of an anomalous redistribution of water mass in the extratropic Pacific during 1998–2002. Geochem Geophys Geosyst 4(11):1096

Chulliat A, Hulot G (2000) Local computation of the geostrophic pressure at the top of the core. Phys Earth Planet Int 117:309–328

Cox CM, Chao BF (2002) Detection of a large-scale mass redistribution in the terrestrial system since 1998. Science 297:831–833

Cox CM, Au A, Boy J-P, Chao BF (2003) Comparison of oceanographic signals with SLR-derived gravity observations. In: Richter B, Schwegmann W, Dick WR (eds) Proc IERS Work-

shop on Combination Research and Global Geophysical Fluids, Bavarian Academy of Sciences, Munich, 18–21 November 2002. IERS Tech Note 30, pp 139–143
Frankfurt am Main: Verlag des Bundesamts für karthographie und Geodäsie, 2003(in print)
Dumberry M, Bloxham J (2003) Variations in Earth's gravitational field caused by torsional oscillations in the core. Geophys Res Abstr 5:05888
Dziewonski AM, Anderson DL (1981) Preliminary reference Earth model PREM. Phys Earth Planet Int 25:297–356
Fang M, Hager BH, Herring TA (1996) Surface deformation caused by pressures changes in the fluid core. Geophys Res Lett 23(12):1493–1496
Forte A, Mitrovica JX (2001) Deep-mantle high-viscosity flow and thermochemical structure inferred from seismic and geodynamic data. Nature 410(6832):1049–1056
Gire C, Le Mouël JL (1990) Tangentially geostrophic flow at the core–mantle boundary compatible with the observed geomagnetic secular variation: the large-scale component of the flow. Phys Earth Planet Int 59(4):259–287
Greff-Lefftz M, Legros H (1995) Core–mantle coupling and viscoelastic deformations. Phys Earth Planet Int 90(3–4):115–135
Greff-Lefftz M, Legros H (1997) Some remarks about the degree one deformations of the Earth. Geophys J Int 131:699–723
Greff-Lefftz M, Legros H, Dehant V (2000) Influence of the inner core viscosity on the rotational eigenmodes of the Earth. Phys Earth Planet Int 122(3–4):187–203
Gubbins D, Roberts P (1987) Magnetohydrodynamics of the Earth's core. In: Jacobs JA (ed) Geomagnetism. Academic Press, London, pp 1–183
Hinderer J, Legros H (1989) Elasto-gravitational deformation, relative gravity changes and Earth dynamics. Geophys J 97:481–495
Hulot G, Le Mouël J-L, Jault D (1990) The flow at the core–mantle boundary; symmetry properties. J Geomag Geoelectr 42(7):857–874
Hulot G, Eymin C, Langlais B, Mandea M, Olsen N (2002) Small-scale structure of the geodynamo inferred from Oersted and Magsat satellite data. Nature 416:620–623
Jault D (2003) Electromagnetic and topographic coupling and LOD variations. In: Jones CA, Soward AM, Zhang K (eds) Earth's core and lower mantle. Taylor & Francis, London, pp 56–76
Jault D, Gire C, Le Mouël (1988) Westward drift, core motions and exchanges of angular momentum between core and mantle. Nature 333:353–356
Le Mouël JL (1984) Outer core geostrophic flow and secular variation of Earth's magnetic field. Nature 311:734–735
Pais A, Hulot G (2000) Length of day decade variations, torsional oscillations and inner core superrotation; evidence from recovered core surface zonal flows. Phys Earth Planet Int 118(3–4):291–316
Reigber Ch, Balmino G, Schwintzer P, Biancale R, Bode A, Lemoine J-M, Koenig R, Loyer S, Neumayer H, Marty J-C, Barthelmes F, Perosanz F, Zhu SY (2002) A high quality global gravity field model from CHAMP GPS tracking data and accelerometry (EIGEN-1S). Geophys Res Lett 29(14):doi:10.1029/2002GL015064
Roberts PH, Scott S (1965) On analysis of the secular variation. J Geomag Geoelectr 17:137–151
Sabaka TJ, Olsen N, Langel RA (2002) A comprehensive model of the quiet-time, near-Earth magnetic field; phase 3. Geophys J Int 151:32–68
Sabaka TJ, Olsen N, Purucker ME (2004) Extending comprehensive models of the Earth's magnetic field with Oersted and CHAMP data. Geophys J Int 159:521–547